AUTOMATIC EXTRACTION OF URBAN STRUCTURES BASED ON SHADOW INFORMATION FROM SATELLITE IMAGERY

Nada M. Mohammed Kadhim[1, 2], Monjur Mourshed[1], Michaela Bray[1]
[1]School of Engineering, Cardiff University, Cardiff, UK
[2]School of Engineering, University of Diyala, Diyala, Iraq
MohammedSalihNM, MourshedM, BrayM1 @ cardiff.ac.uk

ABSTRACT

The geometric visualisation of the buildings as the 3D solid structures can provide a comprehensive vision in terms of the assessment and simulation of solar exposed surfaces, which includes rooftops and facades. However, the main issue in the simulation process for accurately assessing buildings' surfaces is a genuine data source that presents the real characteristics of buildings. This research aims to extract the 3D model as the solid boxes of urban structures automatically from Quickbird satellite image with 0.6 m GSD for assessing the solar energy potential. The results illustrate that the 3D model of building presents spatial visualisation of solar radiation for the entire building surface in a different direction.

INTRODUCTION

Providing sufficient energy to meet the needs of urban dwellers is undoubtedly a challenging task. Solar energy is one form of clean renewable energy that can provide sustainable electricity without toxic pollution or global warming emissions. Therefore, there is a growing demand worldwide for the use of solar photovoltaic (PV) technology because it has a much lower environmental impact than other conventional energy sources. However, in order to exploit this renewable energy within urban areas, a crucial process is the automated detection and evaluation of the surfaces available for integrated solar installations. In particular, the simulation of roof/surface brightness from a genuine source that presents the real characteristics and functionalities of buildings still remains an open issue. Further, although considerable research has been devoted to detecting the rooftops of buildings, rather less attention has been paid to creating and completing a 3D model of urban buildings. For this reason, there is a need to increase our understanding of the solar energy potential of surfaces and roofs to formulate future adaptive energy policies for the sustainability of cities.

This paper is devoted to the automated extraction of 3D urban structures as solid blocks using Very High Resolution (VHR) satellite imagery. The motivation to use VHR satellite imagery is that such data can provide reliable and efficient detail in the creation of urban buildings within various urban landscapes. Furthermore, satellite imageries can provide a magnificent test domain for any application with a variety of illumination and environmental conditions, and can be available in the public-domain (e.g. Google Earth). Satellite images are useful for locating individual buildings, connected buildings, and both small and large buildings, providing information about their geometry, and depicting the surrounding environment of buildings and the urban fabric nearby. Therefore, we focus on assessing the solar energy potential not only of the rooftops but also the buildings' surfaces in VHR satellite image acquired from urban area which solely contains the detached buildings through the automatic creation of a 3D vision of these buildings.

Many previous studies in this context have evaluated the amount of insolation within urban areas on diverse data types, such as pre-existing maps of building footprints, LiDAR data, and/or aerial images. However, such data has proven its effectiveness in solar energy assessments within urban landscapes, even though the availability of such data in a particular urban area is mostly difficult to obtain. This is due to, for instance, their high costs (e.g. LiDAR and aerial images) or not being frequently updated (e.g. the building footprint maps). The production of the building location maps requires continued survey campaigns, which also require more money, time and effort. Such data and maps cannot even be collected if there is a conflict within a study area or access is difficult. However, such cases have quite commonly collected real geospatial data to assess the solar energy potential for feeding the existing buildings with sufficient electrical energy as one form of solar energy utilisation. VHR satellite imageries are a good alternative to overcome the difficulty of collecting data from a genuine data source at lower cost, with continuous updating, and a wide area of coverage. In addition to the availability of visible bands (R, G, and B) in a VHR satellite image, the near-infrared band (INR) is an important spectral band that can be used to extract the shadow regions of buildings, which are considered strong evidence of the existence of urban constructions.

In this paper, we propose a new approach which will automatically create 3D models of isolated buildings from a VHR multispectral satellite image without any extra information. The proposed approach of the

vision of 3D buildings as solid blocks/boxes helps us to maximise the ability to exploit the solar energy potential in a city. The generated 3D model of urban structures can also be used later for further solar energy utilisation and analysis. The approach considers the real locations of detached buildings and the estimated heights of these buildings from VHR satellite images. To implement the proposed approach, we use Quickbird (0.6 m GSD) with four spectral bands (R, G, B and INR), the study area being in Ankara, Turkey. Thereafter, we export 3D models to the Ecotect software and simulate the calculation of the total monthly solar exposure of the buildings' rooftops and side surfaces (walls).

The remainder of this paper is organised as follows. Previous studies are summarised in Section 2. The proposed approach is presented in Section 3. The evaluation of the 3D model of urban structures are given in Section 4. The assessment of solar energy potential is reported in Section 5. The results and discussion are illustrated in Section 6. The conclusion and future directions are provided in Section 7.

PREVIOUS WORK

The automated creation of 3D objects from images is an open research area of image processing and computer vision as well as remote sensing. In particular, the extracted 3D object which represents an urban structure (e.g. buildings) can be used to evaluate the availability of their surfaces for integrated solar installations; exploiting such renewable energy is a crucial assessment process. Many pioneering studies for the assessment of rooftop PV potential were devoted to taking advantage of the potential of solar energy through investigating the availability and suitability of the rooftops of buildings. Based on modified solar-architecture rules of thumb, Peng and Lu (2013) estimated the PV-suitable rooftop area from a building's ground floor area. As stated by their method, the gross roof area is computed based on using a gross roof area vs. ground floor area ratio. Thereafter, solar suitability and architectural factors are used to calculate the potential PV-suitable rooftop area of two kinds of buildings: hotel and commercial, which is estimated at 54 km2 and with 5981 GWh as the predicted annual potential energy output. Another approach to evaluate the supply of solar energy to building rooftops (residential buildings) is based on the use of LiDAR data, introduced by Tooke et al. (2011). The approach contains Kernel window moving and thresholding methods to extract vegetation cover and buildings from a digital surface model (DSM). The calculation of the attributes in this approach, such as height and volume from DSM, sought to investigate the solar radiation received by building rooftops. The total solar radiation received by residential buildings will be decreased by around 38% because of urban structures, due to the influence of trees. Singh and Banerjee (2015) presented a method for estimating the rooftop solar PV potential of a region based on various data (e.g. land use maps, Google Earth images, and climate data), and different tools (e.g. GIS and PVSyst simulation) with multiple strategies of analysis. The extraction of the total rooftop area available for PV installation is achieved by calculating the total Building Footprint Area (BFA) with the Photovoltaic-Available Roof Area (PVA) ratio applied on sample buildings through micro-level simulations using PVSyst. The estimated rooftop solar PV potential represents 2190 MW with an annual average capacity factor of about 14.8%. Because the amount of sunlight is a crucial factor of solar PV efficiency, Ko et al. (2015) evaluated the potential of solar PV power generation on rooftops. The approach was based on an analysis of building GIS layers (coordinates and stories) using a Hillshade module. A raster binarisation map was combined with hourly sun shadow greyscale values (including the solar azimuth and elevation angles of buildings), to distinguish bright and dark patches for computing roof shadow area. The results indicate about 12,428.5 MW as the rooftop solar PV installation capacity with a power generation capacity of 15,423.75 GWh. The process of assessing the available solar radiation on the rooftops in the aforementioned studies was completely reliant on the existence of urban structure maps that may pose a problem in other study areas in which such maps are not available.

Many researchers have developed strategies that deal with the evaluation of urban structures by different applications, such as solar energy utilisation from VHR aerial/satellite images. Bergamasco and Asinari (2011) proposed an approach to calculate the available roof surface for solar energy utilisations based on the systematic analysis and processing of aerial georeferenced images. In a different work, Kabir et al. (2010) attempted to recognise bright rooftops by classifying Quickbird images to estimate solar energy for PV application. Discrimination between rooftops and non-rooftops was achieved by Baluyan et al. (2013), using image segmentation based on machine learning namely: k-means clustering and support vector machines (SVM). The automated detection of different building structures through exploiting the shadow presence in VHR multispectral satellite images was proposed by Ok (2013). Because shadows in VHR satellite images can provide evidence of man-made structures, shadows are a key factor in the analysis of solar radiation across daylight (Kadhim et al. 2015). In this regard, the estimation of the available rooftop area for PV installation was implemented by Jo and Otanicar (2011), who analysed the patterns of shadow cast and its effects on the rooftops.

The derived shadow information from VHR satellite images has been used for other purposes in addition to solar energy assessment, such as the estimation of building heights and the evaluation of the creation and visualisation of buildings as 3D models. Building height extraction (Lee and Kim 2013; Raju et al. 2014), and estimation of 3D models of buildings (Izadi

and Saeedi 2012) were also tested based on shadows and acquisition geometry from VHR satellite images.
A major problem of the above approaches is that the extraction of building heights, footprints and 3D frames from the tested images has mostly focused on: height adjustment for matching the projected buildings with their shadows; example- and rule-setting for extracting the rooftops and shadows; and, a hypothesis for defining 2D rooftops to estimate 3D buildings, where such rules and hypotheses are limited to the selected images and cannot be generalised to buildings with different geometric properties and on the captured VHR images with diverse conditions.
Interestingly, the calculation of the roofs and facades as a solar 3D urban structure model has been taken into consideration by two recent studies. Redweik et al. (2013) developed an approach to assess the solar energy potential of buildings based on the calculation, visualisation and integration of the potential of both building roofs and facades using LiDAR data (DSM) and a solar irradiation model based on climatic observations. The results of the solar 3D buildings analysis confirmed that the annual irradiation on vertical facades is lower than roofs. The spatio-temporal analysis has been conducted for solar irradiation assessment on building roofs and vertical facades by Catita et al. (2014), using three different datasets: a solar radiation model for roofs, ground and facades; a 3D building model; and a DSM from LiDAR data fused in a GIS environment. The developed approach presents the assessment of multiple buildings with the details of the individual unit area at one end. However, the two approaches require the availability of DSM derived from airborne LiDAR data, which is a serious problem if we consider that the assessment of solar energy potential covers an entire city or large area of urban landscape.

METHODOLOGY

The proposed approach is summarised in the workflow shown in Figure 1. The whole process of implementation can be broken down into the following five interrelated sections. The new method uses a VHR single multispectral image to derive a building shadow map as a binary image in the first part. Thereafter, this binary image is post-processed with the original image to collect the coordinates of the corners of every building. The approach derives the estimation of building height from the building shadow map. The gathered coordinates and the derived heights of the buildings are used to create a 3D model of urban structures as solid boxes which represent the location of the existence of buildings in the VHR satellite image. The last step assesses the solar energy potential of the created 3D model of urban structures. The five stages of the method are described in the subsequent sections.

Shadow detection

To extract the shadow regions of urban structures from the Quickbird image (0.6 m GSD), we take advantage of the four band multispectral Quickbird image (NIR band) to compute ratios between the near-infrared (NIR) and visible bands on a pixel-by-pixel basis. This allows the automatic calculation of a binary shadow mask. To this end, we adopted one of the current state-of-the-art shadow detection algorithms, which is the ration-band algorithm published by Rufenacht et al. (2014). The work basis of the ration-band algorithm depends on two main observations: the dark objects in the visible spectrum are much brighter in NIR, and the illumination behaviour of the shadow regions with their surroundings can be better observed in NIR. The shadow candidate map (D) and the ratio image (T) in the algorithm in Figure 1 are derived by applying a non-linear mapping function on the VHR image. The two results then become able to discriminate between a dark object and an actual shadow, even if the pixel values in both the visible (R, G, and B) and NIR for a given object are dark. Thus, the range of both D and T are located between [0,1] and, on this basis, the elements of the shadow map u_{ij} have been calculated as follows:

$$u_{ij} = \left(1 - d_{ij}\right)\left(1 - t_{ij}\right) \quad (1)$$

An accurate binary shadow mask is attained using the thresholding process. The method in Rufenacht et al. (2014) illustrates in detail the processing steps of the automatic shadow detection and parameter rationales. However, the ratio-band algorithm has been applied to a non-satellite image. To apply the ratio-band algorithm to the Quickbird image (the test image), we adopted our pervious refinement method, as presented by Kadhim et al. (2015). The obtained outcomes are provided in Figure 2, using the implementing ratio-band algorithm on the Quickbird image.

Building corners collection

In this stage of the approach, the coordinates of the corners of every isolated building are gathered. The aim of the collection process of the corner points is to identify the main geometry of urban structures. To this end, the tracing object boundaries technique is applied to the obtained binary shadow image to determine the building boundary, as the first step. Next, the tracing of the building corners is implemented based on every building structure boundary of the building. Four corner points are automatically extracted by deriving the spatial coordinates of the presence of the building structure (X and Y coordinates) within the image space, and each point of the building's corners are labelled in the test image in Figure 3. The coordinates were stored as a matrix with the accuracy of every corner of the detached buildings in the Quickbird image. The evaluation of the correct location for the building corners was achieved compared to the reference data consisting of building corners, which were produced manually, using the well-known Root Mean Square Error (RMSE) in Table 1.

The estimation of heights of urban Structures

To automatically generate the 3D model of urban structures from the VHR satellite image, the height of

the building (the Z Dimension) is required. The goal of the third post-processing step applied to the binary shadow building image is to estimate the height of the urban structures (the detached buildings). We investigated the length of each shadow region in the direction of illumination and the geometry of the shadow pattern itself in Figure 4. The computation was implemented based on a flat terrain assumption with assuming the image is captured with a nadir angle. This fundamental assumption takes into account the direct trigonometric relation between shadow length and urban structure height was used by Ok et al. (2013) and Ok (2013) as the basis for estimating the heights of buildings. We built an interactive tool in the form of a Graphical User Interface (GUI) to measure the length of the Z-dimension and then multiply by the number of pixels to calculate the model height using the following formula:

$$H_B = L_{Sh} * P_{ij} \quad (2)$$

Where, H_B is the height of the urban structure, L_{Sh} is the measured length from each shadow region with the direction of illumination, and P_{ij} is the number of measured pixels in the image space. The outcomes were then compared to the building height calculator that computes the building heights based on the Sun Elevation Angle value and the distance between the edge of the building object and the cast edge of shadow for the given building using RMSE, which are available as shown in Table 2.

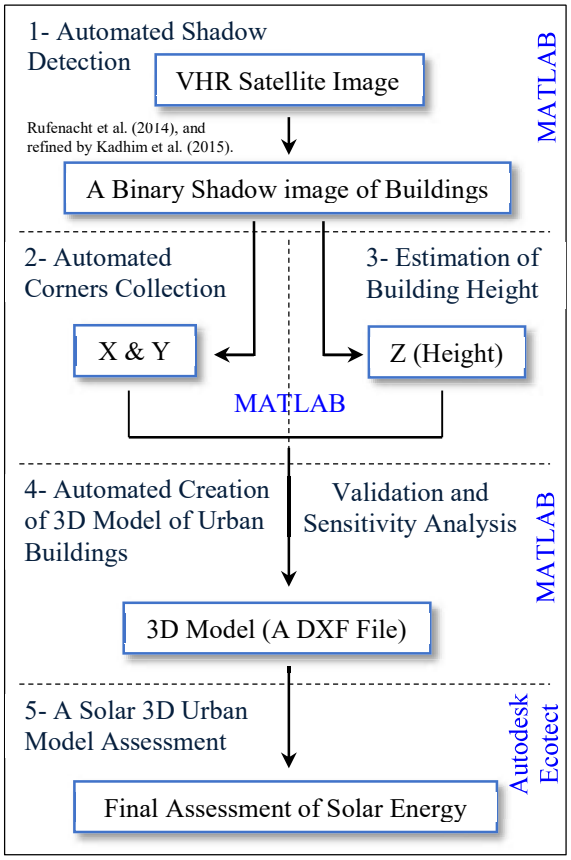

Figure 1 Workflow of the proposed Approach

Automated Creation of a 3D Model of Buildings

Once the coordinates of the buildings' corners were determined and the heights from the shadow regions of these buildings estimated and derived. The construction stage of the 3D geometry as solid boxes was implemented for each isolated building. We automatically extracted 3D urban structures based on generating polygons using the location of buildings and their heights. Thereafter, the constructed polygons were connected by accomplishing the arithmetical procedures between the angles and vertices of these polygons, as in Figure 5. The tagged data function was created to save the outputs as a DXF format in order to use this output file, which includes 3D solid geometry of each building as an input file for assessing the solar energy potential for urban structures. Sensitivity analysis in terms of testing the uncertainty in the output of the 3D model was conducted in this fourth stage of our approach in order to evaluate the model and refine it.

The implementation and processing of the aforementioned four stages of the new proposed method was performed in MATLAB. All tests were performed on a computer with an Intel i7 processor with 3.40 GHz and 16 GB RAM.

Assessment of Solar Energy Potential

The purpose of the extraction of the 3D model of urban structures from a 2D image space was to allow the assessment and visualisation of the solar energy potential of buildings, not only for their roofs but also for the rest of the surfaces (walls). In addition, the successful deployment of PV systems in urban environments depends on the highest amount of incident solar radiation which can be spotted on the appropriate space of the building roofs and surfaces at any date, time and location. Therefore, the last stage of the method relates to the assessment and analysis the solar radiation on the surfaces of the extracted 3D geometry of the urban structures. The assessment and simulation processes were implemented in Ecotect software Copyright © 2010, Autodesk, Inc.

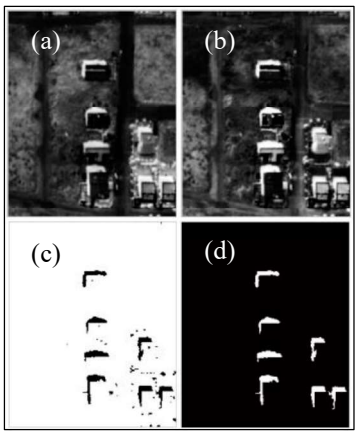

Figure 2 Quickbird image, (a) visible bands, (c) NIR band, (c) Shadow mask, (d) the final result of the shadow mask after enhancing the current algorithm

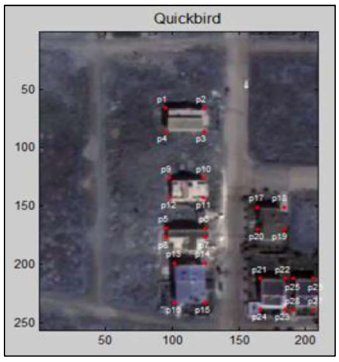

Figure 3 The labels and lcation of the building corners on Quickbird (0.6 GSD) test image

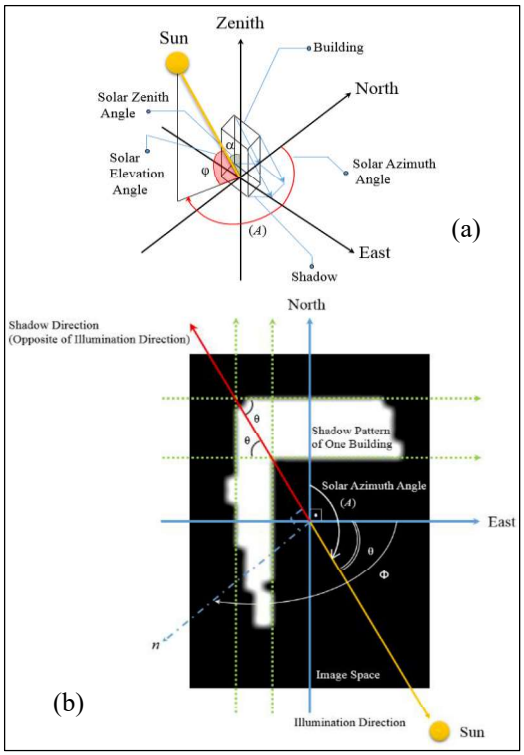

Figure 4 (a) 3D visualisation of solar angles: Sun Elevation, Azimuth and Zenith angle with the formation of a cast shadow of the urban structure, (b) a shadow pattern of the actual illumination direction and its opposite direction, which is composed of the cast direction of the shadow with the geometric angles of the relationships within the image space

THE EVALUATION OF THE 3D MODEL OF URBAN STRUCTURES

To evaluate and test the uncertainty in the creation of a 3D model of detached buildings, we investigated the area of the base (building footprint) of a 3D solid box (which is also the same area of the top of a 3D model). The shape of the buildings mostly represents a rectangle shape, and therefore the area must be a regular rectangular shape. This means the geometry of the 3D solid boxes has right angles in each corner between each of the two edges (in the 2D plan) within the area of the base of the model. Accordingly, the reference data (e.g. the shape of polygon) of each building of test image was manually prepared by a qualified human operator using ArcGIS and their areas were calculated. Essentially, the reference data is the data that was derived from high precision measurements of their field measurements or aerial photography or satellite imagery with a high spatial resolution, including a local coordinate system and widely used for comparison. Thereafter, the comparison was based on an object-based assessment between two area values of the building footprints of the reference and computed area values from the created 3D model were conducted. The results of the comparison are shown in figure 6, which presents some discrepancies between the true and measured values. These discrepancies between the base area of the 3D model (measured value) and the building footprint area of the reference of the geometric building (true value) were taken into account and corrected using Ecotect software.

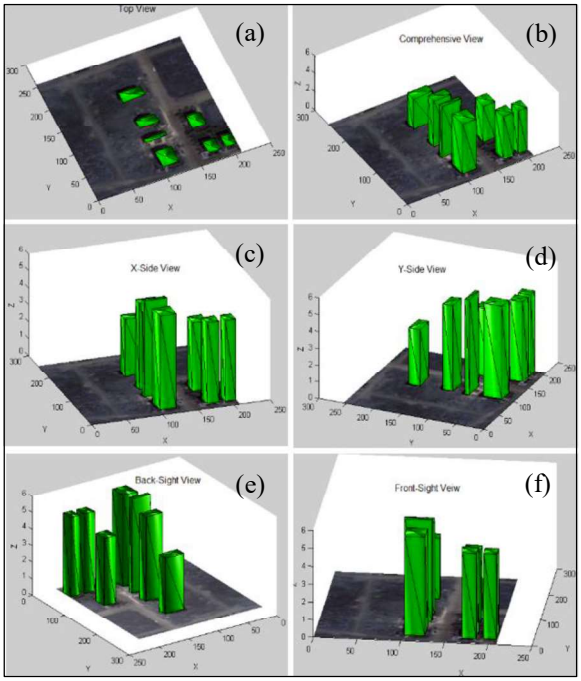

Figure 5 3D model of urban structures results of the proposed approach with different azimuth (Az) and Elevation (El) of MATLAB visualisation, (a) 3D buildings visualised by the top view, (b) Comprehensive view Az:71 & El:28, (c) X-side view Az:-20, El:36, (d) Y-side view Az:-66, El:36, (e) Back-sight view Az:147, El:36, (f) Front-sight view Az:7, El:36

ASSESSMENT OF SOLAR ENERGY POTENTIAL

The verification of the correct geometry is implemented for the 3D model of urban structures in Figure 7a and the true sun path and shadows of buildings in Figure 7b. We consider the climate data to assess, simulate and analyse the solar radiation on building roofs and surfaces in Ecotect software. The assessment is performed in terms of simulation and

calculation of the cumulative values of the incident solar radiation and total monthly solar exposure in Figure 8. The total cumulative solar radiation calculation and simulation were implemented on all surfaces (rooftops and walls) of buildings across every month covering the entire year in different directions. The goal behind this simulation is to calculate and assess the availability of incident solar radiation (insolation) on surfaces within our model. To achieve this goal, we used the weather file of our study area in Ankara, which was created based on hourly recorded data. We also consider the overshadowing and shading calculation for the geometry of the buildings and their surroundings.

Table 1

Performance results of corner detection of buildings from the VHR satellite image (Quickbird test image)

ID	Diff. of Location (Pixels)	Accu. (%)	ID	Diff. of Location (Pixels)	Accu. (%)
1	0	100	15	0	100
2	0	100	16	0	100
3	8.98	91.02	17	0	100
4	2.84	97.16	18	7.25	92.75
5	0	100	19	66.15	33.85
6	0	100	20	65.36	34.65
7	0	100	21	0	100
8	0	100	22	0	100
9	7.40	92.60	23	6.06	93.94
10	3.31	96.69	24	6.06	93.94
11	9.86	90.64	25	0	100
12	7.40	92.60	26	13.80	86.20
13	0	100	27	14.86	85.13
14	0	100	28	5.52	94.48

Table 2

Performance results of the estimation of buildings heights from the VHR satellite image (test image)

No. of buildings	The measured value of building height (m)	The estimated value of building height (m)	Differences M-E (m)
1	3.70	3.40	0.30
2	4.80	5.10	-0.30
3	4.00	5.70	-1.70
4	5.60	5.60	0.00
5	4.00	4.10	-0.10
6	5.60	4.80	0.80
7	5.60	4.80	0.80
RMSE			-0.20
Mean -0.029		Standard Deviation ±0.79	

RESULTS AND DICUSSION

We visualise the assessment of the solar energy potential of urban structures, which are derived from the Quickbird test image in Figure 9. The extraction of the 3D model of urban structures demonstrates that our approach can provide remarkable assessment and quite representative results. The assessment of the solar energy potential for rooftops and facades based on the solar 3D model of urban structures using Ecotect software provides an opportunity to carry out a fair quantitative comparison.

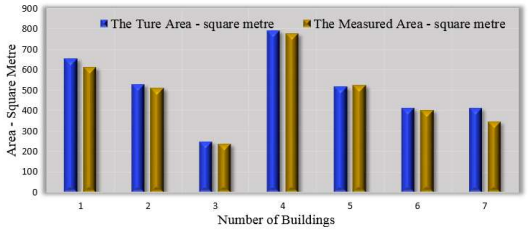

Figure 5 Evaluation of the areas of the polygons of the extracted 3D model of urban buildings and the reference data. The correction was implemented to the extracted areas of the 3D model based on restoring the right angles at the intersection of two perpendicular straight lines

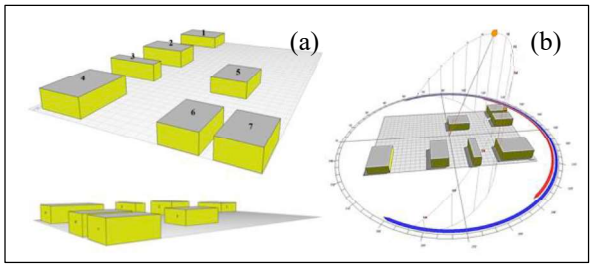

Figure 6 (a) The modified geometry of the 3D model of the detached buildings in Ecotect, (b) the setting of the sun path and the cast shadows of the detached buildings in Ecotect

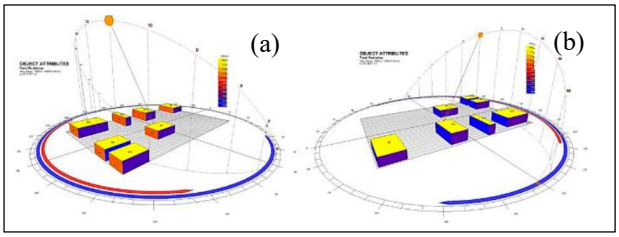

Figure 7 Solar radiation assessment for urban structures (a) in the same direction of the solar radiation, (b) in the opposite direction of the solar radiation

According to Figure 9, the results illustrate the differences between the amount of solar radiation received by buildings' roofs and surfaces (walls). The lower values of incident solar radiation were found within the buildings' facades in the north direction in Figure 9a. The facades in the east and west directions present convergent values of solar radiation whereas the inconsistent values were observed within the facades in the south direction. In contrast, the amount of received solar radiation by rooftops was higher than other surfaces which exhibits large values of insolation due to the fact that the regions of the rooftops were full exposed to sunlight in Figure 10. In particular, because the selected study area lacks dense vegetation cover, such as trees, they receive more solar radiation and thus have less overshadowing vegetation cover over the rooftops.

The results prove that the extracted 3D model of urban structures is generic for solar energy utilities in terms of assessing solar energy potential on all building surfaces. Nevertheless, there was only displacement from the original location of the two corners P19 and P20 in the test image because the colour density of the building roof was similar to its surrounding density colour pixels. This shift in distance between corner positions was corrected during the adjustment of the 3D model using reference data in the final stage before assessing solar energy potential on all surfaces.

In spite of the conducted amendment of the 3D solid boxes, the proposed approach for creating and extracting the 3D model of urban structures allows us to create an immersive environment and deliver results for vertical, horizontal and shaded surfaces. In this regard, the opposite facades of both building six and building seven provide notably different values of solar radiation across the whole year in Figures 9b and 9e. This is because both the two buildings adjacent to each other more than the rest of the buildings. Consequently, the shadow envelope of every two buildings has an impact on each other in terms of the dilution of solar energy that can receive these surfaces in the daily insolation.

The total monthly solar exposure across the whole year was about 166.766 KWh/m2. Further, it is found that the highest total solar radiation value within the selected urban area was about 180.60 KWh/m2 in the July month, 2015. Accordingly, we chose this month to present the differences of incident solar radiation values on all surfaces of the buildings in Figure 10. Façade 13 of building six has the lowest values between other buildings' facades directed towards the ED. Similarly, façade 28 of building seven has also the lowest value compared to the other buildings' facades directed towards the WD. This result confirms the aforementioned results in Figure 9, in that the adjacent buildings with smallest distance between their constructed locations can affect the amount of radiation received by the facades of some buildings nearby. A distinctive property of the proposed approach is that the reconstruction of the 3D geometric model of urban buildings for the solar energy assessment was achieved from the direct utilisation of the source of real data represented in the VHR multispectral satellite imagery, without requiring extra information.

CONCLUSION

In this study, a novel approach was developed for the extraction of the 3D model of urban structures from single VHR multispectral image for the assessment of the solar energy potential within urban environment. The approach was applied to detached urban buildings in Ankara, Turkey. Solar assessment and estimation was performed not only on the buildings' roofs but also on their facades in the different directions using the Quickbird image with a spatial resolution of 0.6 m GSD. We extracted the shadow regions from the test

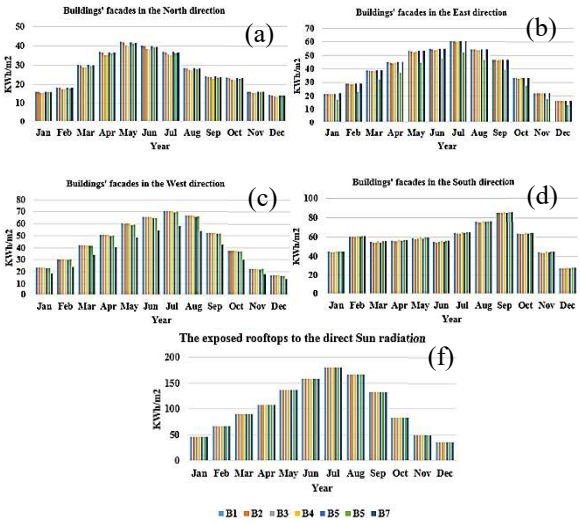

Figure 8 (a) Annual cumulative solar radiation for an exposed surface area of buildings in the north direction, (b) orientated towards the east direction, (c) the south direction, (e) the west direction, and (f) the direct exposure of the rooftops to the solar radiation (from the simulation values)

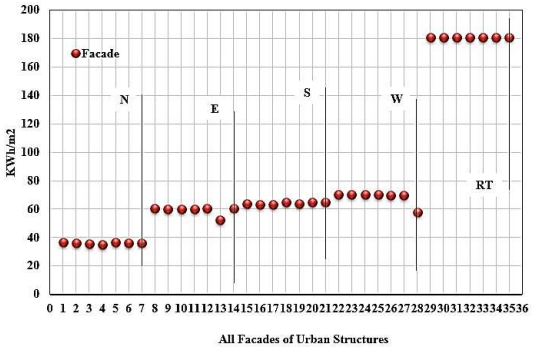

Figure 9 The assessment of all surfaces (roofs and walls) of urban buildings in the study area in the Quickbird test image across one month (July, 2015). In the x-axis (1 - 7) represent the façade numbers of the buildings towards the north direction (N), (8 - 14) towards the east direction (E), (15 - 21) towards the south direction (S), (22 - 28) towards the west direction (W), and finally (29 - 35) represent rooftops (RT)

image in order to estimate the building heights. A cast shadow and its presence in satellite images provides useful information to verify the existence of a building structure with a certain geometric configuration. Then, we detected the corners of the buildings to determine their geometry and shape. Thereafter, the automated algorithm for the extraction of the 3D model of buildings was implemented as the solid boxes in Matlab to represent the urban structures in the test image. The 3D model enables us to have a comprehensive visualisation of buildings in terms of the assessment of solar energy potential and the impact the building's envelopes on each other even though the study area includes the isolated buildings. The assessment of solar radiation of urban structures

was achieved based on the calculation of the annual cumulative solar radiation values for every surface (rooftops and walls) using climate data implemented in Ecotect software.

It is concluded that the bright facades are not necessarily of less benefit and suitability than rooftops for PV usage despite their low values of insolation. The facades in a good position in relation to the sun can provide a suitable area for PV application in the modern urban landscape. Additionally, the results of the 3D isolated buildings present an ideal situation to receive more solar radiation compared to the adjacent urban structures. The results can be exploited for the development of solar energy utilised policies and urban planning. Therefore, the proposed approach can be an exploratory calculation of solar potential at the municipal level.

In the future, we plan to carry out tests on the dense urban area and vegetation cover using different VHR images. We will focus on enhancing the proposed approach in order to be able to evaluate buildings' facades with the cast shadows from other higher buildings at the highest hour of insolation.

ACKNOWLEDGEMENTS

The authors would like to thank Dr. Ali Ozgun Ok for providing the Quickbird image used in this study.

REFERENCES

Baluyan, H. and Joshi, B. and Al Hinai, A. and Woon, W. L. 2013. Novel approach for rooftop detection using support vector machine. *ISRN Machine Vision* 2013.

Bergamasco, L. and Asinari, P. 2011. Scalable methodology for the photovoltaic solar energy potential assessment based on available roof surface area: Further improvements by ortho-image analysis and application to Turin (Italy). *Solar Energy* 85(11), pp. 2741-2756.

Catita, C. and Redweik, P. and Pereira, J. and Brito, M. C. 2014. Extending solar potential analysis in buildings to vertical facades. *Computers & Geosciences* 66(0), pp. 1-12.

Izadi, M. and Saeedi, P. 2012. Three-Dimensional Polygonal Building Model Estimation From Single Satellite Images. *Geoscience and Remote Sensing, IEEE Transactions on* 50(6), pp. 2254-2272.

Jo, J. H. and Otanicar, T. P. 2011. A hierarchical methodology for the mesoscale assessment of building integrated roof solar energy systems. *Renewable Energy* 36(11), pp. 2992-3000.

Kabir, M. H. and Endlicher, W. and Jägermeyr, J. 2010. Calculation of bright roof-tops for solar PV applications in Dhaka Megacity, Bangladesh. *Renewable Energy* 35(8), pp. 1760-1764.

Kadhim, N. and Mourshed, M. and Bray, M. 2015. Shadow Detection from Very High Resoluton Satellite Image Using Grabcut Segmentation and Ratio-Band Algorithms. *ISPRS-International Archives of the Photogrammetry, Remote Sensing and Spatial Information Sciences* 1, pp. 95-101.

Ko, L. and Wang, J.-C. and Chen, C.-Y. and Tsai, H.-Y. 2015. Evaluation of the development potential of rooftop solar photovoltaic in Taiwan. *Renewable Energy* 76(0), pp. 582-595.

Lee, T. and Kim, T. 2013. Automatic building height extraction by volumetric shadow analysis of monoscopic imagery. *International Journal of Remote Sensing* 34(16), pp. 5834-5850.

Ok, A. O. 2013. Automated detection of buildings from single VHR multispectral images using shadow information and graph cuts. *ISPRS Journal of Photogrammetry and Remote Sensing* 86(0), pp. 21-40.

Ok, A. O. and Senaras, C. and Yuksel, B. 2013. Automated Detection of Arbitrarily Shaped Buildings in Complex Environments From Monocular VHR Optical Satellite Imagery. *Geoscience and Remote Sensing, IEEE Transactions on* 51(3), pp. 1701-1717.

Peng, J. and Lu, L. 2013. Investigation on the development potential of rooftop PV system in Hong Kong and its environmental benefits. *Renewable and Sustainable Energy Reviews* 27(0), pp. 149-162.

Raju, P. and Chaudhary, H. and Jha, A. 2014. Shadow analysis technique for extraction of building height using high resolution satellite single image and accuracy assessment. *ISPRS-International Archives of the Photogrammetry, Remote Sensing and Spatial Information Sciences* 1, pp. 1185-1192.

Redweik, P. and Catita, C. and Brito, M. 2013. Solar energy potential on roofs and facades in an urban landscape. *Solar Energy* 97(0), pp. 332-341.

Rufenacht, D. and Fredembach, C. and Susstrunk, S. 2014. Automatic and Accurate Shadow Detection Using Near-Infrared Information. *Pattern Analysis and Machine Intelligence, IEEE Transactions on* 36(8), pp. 1672-1678.

Singh, R. and Banerjee, R. 2015. Estimation of rooftop solar photovoltaic potential of a city. *Solar Energy* 115(0), pp. 589-602.

Tooke, T. R. and Coops, N. C. and Voogt, J. A. and Meitner, M. J. 2011. Tree structure influences on rooftop-received solar radiation. *Landscape and Urban Planning* 102(2), pp. 73-81.